



Contents lists available at ScienceDirect

## Materials Today: Proceedings

journal homepage: [www.elsevier.com/locate/matpr](http://www.elsevier.com/locate/matpr)

# Effect of montmorillonite clay on the fluorescence resonance energy transfer between two cationic dyes Acridine Orange and Rhodamine B in solution

Utsav Chakraborty, Pradip Maiti, Tanmoy Singha, Ujjal Saren, Alapan Pal, Pabitra Kumar Paul\*

Department of Physics, Jadavpur University, Jadavpur, Kolkata 700032, West Bengal, India

## ARTICLE INFO

## Article history:

Received 5 April 2020

Received in revised form 1 May 2020

Accepted 3 May 2020

Available online xxx

## Keywords:

FRET

Cationic dyes

Rhodamine B

Acridine orange

Fluorescence

Montmorillonite

## ABSTRACT

In this article the Fluorescence resonance energy transfer (FRET) between two important cationic dyes namely Acridine Orange (AO) and Rhodamine B (RhB) in aqueous solution in presence and absence of montmorillonite (MMT) is demonstrated. The energy transfer is also studied in ethanolic solution. Excited state energy migration is occurred from AO to RhB molecules and the extent of energy transfer efficiency linearly increases with increase in RhB concentration in the solution. Interestingly the incorporation of MMT clay significantly increases the energy transfer efficiencies between the dye pair in the solution but the nature of interaction depends on the clay concentrations studied in the present work. The nature of quenching of steady state fluorescence emission of AO in presence of RhB as well as MMT clay in the mixed ensemble is systematically investigated and further confirmed by Time-resolved fluorescence and temperature-dependent steady state fluorescence emission experiments. AO and RhB dye molecules formed ground state complex with MMT clay followed by static quenching. As the clay platelets successfully control the FRET efficiency and it is also well known that MMT clay can host wide diversity of molecular species therefore, the present studies may provide a new insight for the design and the development of FRET-based molecular sensors.

© 2020 Elsevier Ltd. All rights reserved.

Selection and Peer-review under responsibility of the scientific committee of the Third International Conference on Materials Science (ICMS2020).

## 1. Introduction

Fluorescence or Förster resonance energy transfer abbreviated as FRET is an excited state photophysical process which has widespread interest to explore many biological system as well as various molecular recognition processes [1]. It was first described in 50 years ago [1] and recently has drawn great attention among the researchers in various fields of research [2–4]. FRET is a distance-dependent phenomenon by which energy is transferred non-radiatively from an electronically excited molecular fluorophore (donor) to another neighbouring fluorophore (acceptor) by means of intermolecular long range dipole–dipole coupling [5]. That is an oscillating molecular dipole can interact and exchange energy with another dipole having similar resonance frequency. The FRET can be an accurate measurement of molecular

proximity at angstrom order distance i.e. 10–100 Å [6]. The extent of this energy migration between the molecular fluorophores also depends on various parameters namely nature of solvent, microenvironment such as pH, ionic concentration, temperature etc. [7–9]. However, the main pre-requisite for FRET to occur is the sufficient spectral overlap of absorption spectrum of the acceptor and emission spectrum of the donor molecules.

Various interesting nanomaterials play significant role for the control of FRET efficiency between organic materials such as dye molecules [10]. Among those, clay nanoplatelets are already attracted great interest in this direction [7]. These are the inorganic nanolaminates which belong to the smectite group of materials and are most abundant in nature. Clays possess high surface to volume ratio, high cation exchange capacity (CEC) and can support a wide variety of organic compounds [11–13] with their unique physical and physicochemical properties [14]. The clay materials have the specific layered structures and therefore they can easily be exfoliated in aqueous medium to prepare a stable colloidal dispersion [15]. Also it is already reported that clay can efficiently

\* Corresponding author.

E-mail addresses: [pkpaul@phys.jdvu.ac.in](mailto:pkpaul@phys.jdvu.ac.in), [pabitra\\_tu@yahoo.co.in](mailto:pabitra_tu@yahoo.co.in) (P. Kumar Paul).

<https://doi.org/10.1016/j.matpr.2020.05.047>

2214-7853/© 2020 Elsevier Ltd. All rights reserved.

Selection and Peer-review under responsibility of the scientific committee of the Third International Conference on Materials Science (ICMS2020).

control the aggregation behaviour of various cationic organic dye molecules in different environment [13,16]. Therefore, if two dye molecules (acceptor and donor) come close proximity in the host clay surface, they can exchange excited state energy via resonance interaction when excited by a light of suitable wavelength [17]. Some researchers found that FRET efficiency between organic dyes organized in Langmuir-Blodgett films was enhanced in presence of clay nanosheets [18]. However, the aggregation of dye molecules on the clay surface may reduce the rate of energy transfer due to reduction in monomeric emission of the donor and acceptor molecules.

In this present article, we have systematically studied the FRET process between two important cationic dyes namely Acridine Orange (AO) and Rhodamine B (RhB) in aqueous medium as well as ethanol solution. The effect of nanoclay montmorillonite (abbreviated as MMT) on the FRET efficiency between AO and RhB in an aqueous environment is also explored. MMT is a well-studied clay and belongs to the class of 2:1 phyllosilicates i.e. smectite type of clay. This type of clays is formed by one octahedral sheet sandwiched between the two tetrahedral sheets per clay layer and sheets contain various exchangeable cations within their layered structures. Other commonly used smectites are laponite, saponite etc. [18] but MMT is differentiated by isomorphous substitution of  $Al^{3+}$  ions in the inner octahedral sheet for  $Mg^{2+}$ . AO and RhB are highly fluorescent and suitable for FRET process to occur as the fluorescence emission of AO shows sufficient spectral overlap with the optical absorption spectrum of RhB and it therefore enables their resonance interaction after photoexcitation in mixed solution. The excitonic energy transfer between these organic dyes has already been demonstrated elsewhere [19], however, the effect on MMT clay on the FRET process for AO-RhB dye pair is not yet studied as far as our knowledge is concerned. The quantitative determination of energy transfer efficiency as a function of MMT clay concentration is studied by means of UV-Vis absorption and steady state fluorescence emission spectroscopy. Also the nature of quenching and the binding of dye molecules on the clay surface is further studied by Time-resolved Fluorescence study and temperature dependent fluorescence emission technique respectively.

## 2. Experimental

### 2.1. Materials

Acridine Orange (AO), Rhodamine B (RhB) and montmorillonite clay (MMT) powder were purchased from Aldrich Chemical Co., USA and were used without further purification. However, their purities were checked by UV-vis absorption and FTIR techniques before use in the experiment. The surface area of the clay is around  $250\text{ m}^2/\text{g}$ . Triple distilled deionized Milli-Q water (Resistivity  $\sim 18.2\text{ M}\Omega\text{-cm}$ ) was prepared by Type-II Lab water purification system (Synergy Plus equipped with Elix Advantage, Millipore SAS, France) and was used to prepare all the aqueous solution for the experiment. Desired amount of MMT clay was dispersed on to Milli-Q water in a beaker and then was rigorously stirred by a magnetic stirrer at ambient condition for 48 h. The clay aqueous dispersion was also subsequently ultrasonicated prior to their use for spectroscopic measurements.

### 2.2. Characterizations

UV-vis absorption and steady state fluorescence emission spectra of the samples were recorded using rectangular quartz cells of 1 cm path length by means of a dual beam absorption spectrophotometer (UV 1800, Shimadzu, Japan) and fluorescence spectrophotometer (Fluoromax-4C, Horiba scientific incorporated, USA),

respectively. For fluorescence emission measurements both the excitation and emission slit-widths were maintained at 2 nm throughout the experiment. For temperature-dependent fluorescence studies, the samples were placed at the sample compartment which is connected to a computer-controlled Horiba make Peltier system to vary the temperatures. Time-resolved fluorescence measurement was carried out by the time-correlated single-photon counting (TCSPC) method using a Horiba Jobin Yvon make time-resolved spectrophotometer (Fluorolog-3) to obtain the fluorescence lifetime data in aqueous environment. The samples were excited at 425 nm using a picosecond diode laser. The typical full width at half-maximum (FWHM) of the system response is about 238 ps. The channel width is 12 ps/channel. The fluorescence decay data were collected over 200 channels which were calibrated on a non-linear time scale with increasing time according to an arithmetic progression with a Hamamatsu photomultiplier tube (R928P). The raw decay curves were deconvoluted and fitted using IBH DAS6 software. The goodness of fit has been assessed over the full decay including the rising edge with the help of statistical parameters  $\chi^2$  and Durbin Watson (DW).

## 3. Results and discussions

### 3.1. UV-Vis absorption and Steady-State fluorescence studies

Fig. 1 shows the area-normalized UV-Vis absorption and steady state fluorescence emission spectra of both AO and RhB dyes in aqueous solution respectively. The molecular structures of the dyes used in this work are shown in the inset of Fig. 1. Pure AO solution gives strong monomeric absorption band at around 490 nm along with a very weak shoulder centered at 470 nm and is consistent with the results reported elsewhere [20,21]. The weak shoulder at 470 nm is due to the presence of some dimeric species of AO molecule but their mean number should be very less compared to dye monomers at very low concentration of solution although they can increase with concentration as already previously reported in the literature [20]. The fluorescence emission spectra (curve 2) gives the characteristic monomeric emission band maximum at around 525 nm after photoexcitation at the wavelength of 425 nm. On the other hand, absorption spectrum of RhB (curve 3) shows the characteristic monomeric band with peak at around

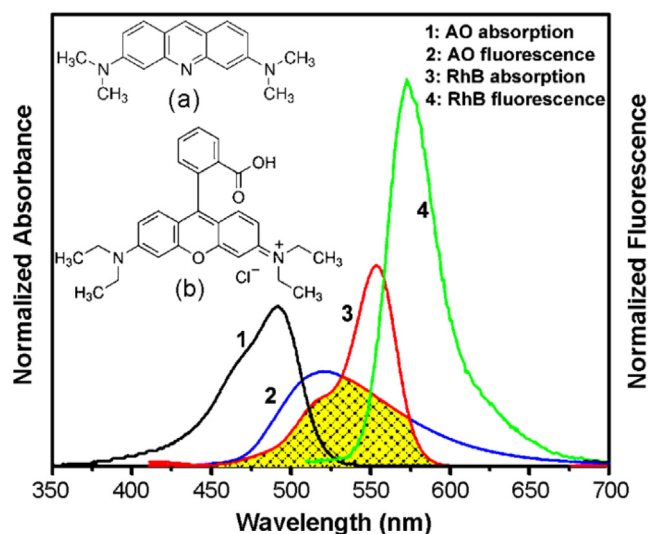


Fig. 1. Spectral overlap between fluorescence emission spectrum of AO and UV-vis absorption spectrum of RhB. Inset shows the chemical structure of (a) AO and (b) RhB.

575 nm which is due to the transition of 0–0 electronic vibrational states and a weak hump at around 520 nm. This weak hump is basically ascribed to 0–1 vibronic transition [22]. However, the manifestation of their molecular interactions are associated with the blue or red shift of the absorption bands as already reported in the literature [23]. Depending upon the nature of interactions and their relative orientation, H- or J-type molecular dimers are formed corresponding to the predominance of absorption band intensity at 531 nm.

From Fig. 1 it is also interesting to note that the emission spectrum of AO and absorption spectrum of RhB has sufficient spectral overlap which is an initial prediction of the possibility of Förster resonance energy transfer (FRET) between them. That is AO can act as donor to transfer its excited states energy to RhB molecules which is presumed as the acceptor molecules for this type of non-radiative energy migration. However, the other factors such as relative distance (1–10 nm) between the donor and acceptor molecules, nature of the surrounding solvent medium etc. are also important criteria for FRET to occur between the fluorophores.

### 3.2. FRET study between AO and RhB in solution

To investigate the excited state energy migration from AO to RhB dye molecules via FRET the fluorescence emission spectra of AO, RhB and their mixed aqueous solution were recorded. The donor molecules (AO) was excited at 425 nm in order to minimize the direct excitation of acceptor molecules (RhB). That is a negligibly small fraction of RhB molecules might have excited at such wavelength. Fig. 2A shows the fluorescence emission spectra of pure AO aqueous solution along with that of AO/RhB mixed (1:1 vol ratio) aqueous solution for various concentration of RhB at fixed pH of 7.0 of the solvent medium. The concentration of AO in the mixed solution was constant i.e.  $5 \times 10^{-6}$  M in all the cases. The emission band observed at 525 nm as shown in the figure (see dashed curve) is originated from AO monomeric species present in the solution. But interestingly the intensity of this band decreases gradually for AO/RhB mixed solution (with increase in RhB concentration) when compared to the emission band of RhB dye monomers in the mixed solution. This sequential quenching of fluorescence emission intensity of 525 nm band (AO) is possibly due to the excited state energy transfer via a non-radiative process

i.e. FRET from excited AO molecules to RhB molecules as there was sufficient overlap between the absorption spectrum of RhB and emission spectrum of AO in aqueous solution. However, this excited state interaction also depends upon the relative orientation of the molecular dipoles and distance between the dye monomer units in the solution after excitation by a suitable wavelength. During photoexcitation, the excited dipoles of AO interacts with RhB molecules which receives energy from electronically excited AO molecules due to long-range dipole–dipole interaction. This eventually results an increase of excited states energy of RhB molecules leading to the enhancement of steady state fluorescence intensity of the band at 575 nm (Fig. 2) in the mixed solution.

To confirm the resonance interaction between the individual excited molecular dipoles of AO and RhB, the excitation spectrum of AO/RhB mixed solution was recorded (figure not shown) while monitoring the fluorescence emission at wavelengths of 525 nm and 575 nm. It was observed that this excitation spectrum was more or less similar to that of pure AO excitation spectrum which also resembles the absorption bands of AO monomers. This study further confirms that the increase of fluorescence intensity at 575 nm was possibly due to the migration of excited state energy of AO to RhB molecules via a resonance interaction between them. To quantify such a non-radiative energy transfer with sequential increase in acceptor (RhB) concentration, we have outlined here some fundamental theoretical consideration. The first quantitative explanation behind the FRET process was proposed by Förster [24] based on some initial idea of dipole–dipole interaction as suggested by Perrin [25]. The rate of this non-radiative energy transfer according to Förster may be written as:

$$k_T = \frac{1}{\tau_D} \left( \frac{R_0}{r} \right)^6 \quad (1)$$

where  $R_0$  is the Förster distance and it depends on the spectral overlap area of the donor emission and acceptor absorption spectrum.  $k_T(r)$  is the energy transfer rate,  $\tau_D$  is the fluorescence lifetime of donor and  $r$  is the distance between donor and acceptor for a particular donor–acceptor pair at any given condition.  $r = R_0$  corresponds to the energy transfer efficiency as 50% and the fluorescence emission of donor would become 1/2 of its initial intensity in absence of the acceptor molecules. The Förster radius  $R_0$  is defined by the following equation:

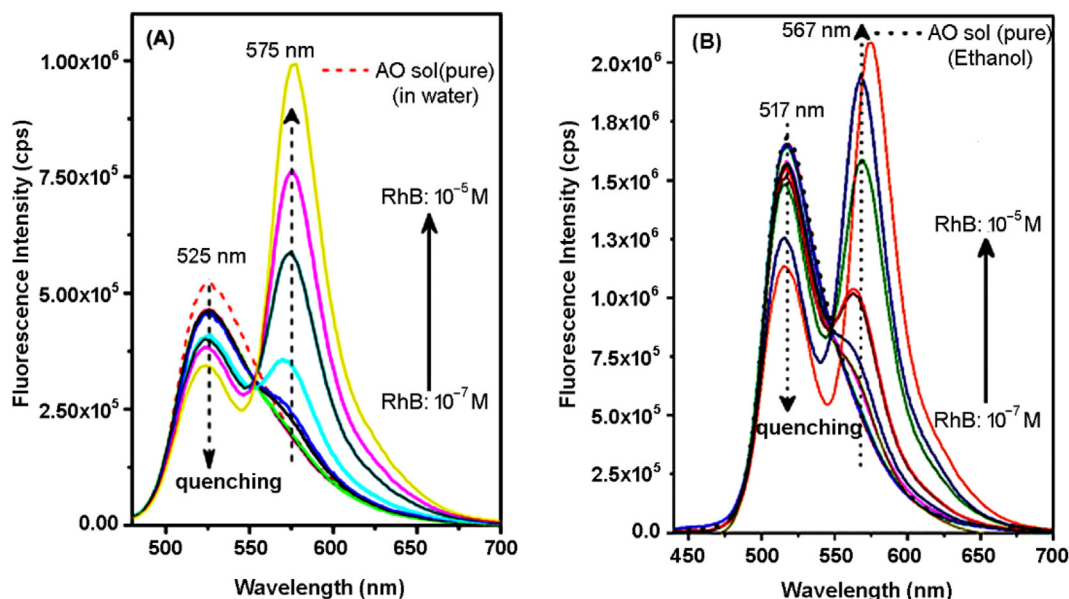


**Fig. 2.** Steady state fluorescence emission spectra of pure AO, and AO/RhB mixed solution (1:1 vol ratio) in water (A) and ethanol (B) with different concentrations of RhB. Concentration of AO was  $5 \times 10^{-6}$  M and was constant for all the mixed solutions.

$$R_0^6 = \left[ \frac{9000(\ln 10)k^2\phi_D}{128\pi^5 N n^4} \right] \int_0^\infty F_D(\lambda)\epsilon_A(\lambda)\lambda^4 d\lambda \quad (2)$$

Where  $F_D$  is the normalized fluorescence intensity of the donor molecules at any particular concentration for which FRET is occurred.  $\epsilon_A(\lambda)$  is the molar extinction coefficient of the acceptor,  $\lambda$  is the wavelength in nm.  $\phi_D$  is the fluorescence quantum yield of the donor (AO in our study),  $n$  being the refractive index of the medium of solution,  $k$  is the orientation factor of the transition dipole moment for the interaction between donor and acceptor molecules;  $N$  is the Avagadro number.

The amount of energy transfer is also dependent on the extent of spectral overlap integral,  $J(\lambda)$  which is basically the integral part of Eq. (2) i.e.

$$J(\lambda) = \int_0^\infty F_D(\lambda)\epsilon_A(\lambda)\lambda^4 d\lambda \quad (3)$$

Therefore, the expression for  $R_0$  can now be written as:

$$R_0 = 0.2108 \left[ k^2 n^4 \phi_D J(\lambda) \right]^{1/6} \quad (4)$$

where  $R_0$  is expressed in units of Å.

The FRET efficiency can be written as:

$$E = \frac{k_T(r)}{k_T(r) + \tau_D^{-1}} = \frac{\tau_D k_T(r)}{1 + \tau_D k_T(r)} \quad (5)$$

The excited donor molecules may be deactivated in number of photophysical pathways i.e. collision, thermal dissipation, energy transfer, electron or proton transfer etc. So equation (5) is basically the fraction of the transfer rate to the total deactivation rate of the donor. From equation (1) and (5) the expression of  $E$  is defined as:

$$E = \frac{R_0^6}{R_0^6 + r^6} \quad (6)$$

We can also write an equivalent equation for the efficiency FRET between donor and acceptor as:

$$E = 1 - \frac{F_{DA}}{F_D} \quad (7)$$

where  $F_{DA}$  is the relative fluorescence emission intensity of donor molecules when mixed with acceptor molecules at a particular concentration and  $F_D$  is that in absence of acceptor molecules in the same medium.

The fluorescence quantum yield  $\phi_D$  of the donor fluorophores in absence of acceptor are estimated using standard theory as already published elsewhere [26].  $\phi_D$  for AO is calculated as 0.27 in aqueous solution and is consistent with the previously reported results [27]. The orientation of the transition dipole moment between donor and acceptor is also an essential factor for the fluorescence quenching of donor via FRET as described earlier. This factor actually depends upon the angle between the transition dipole moment of donor and acceptor molecules as well as the angle between these two dipole moments with the line joining their centres [28].

Therefore, using the above theoretical consideration the FRET efficiency along with all other FRET parameters for AO-RhB dye pairs have been estimated and is summarized in Table 1.

We have also studied the FRET between AO and RhB using ethanol as the solvent. Ethanol is less polar compared to water and therefore it is anticipated that it might have some direct impact on the FRET process between these two cationic organic dyes. Fig. 2B shows fluorescence emission spectra of mixed ethanolic solution of AO and RhB along with that of the pure AO. Concentrations of AO and RhB were same as in the case of FRET study in aqueous environment. The fluorescence emission spectrum of pure AO in ethanol solution shows the intense monomeric peak at

around 517 nm which is somewhat blue shifted compared to that in aqueous solution. The excitation wavelength was 425 nm. This shift of fluorescence spectrum may be attributed to an excitation in the lowest excited singlet states in the photoexcited molecules with relatively greater dipole moment than the ground electronic states. It is also evident from Fig. 2B that with increase in RhB concentration in the mixed solution the emission intensity at 517 nm is gradually decreased with sequential increase of emission band intensity at 567 nm. These observations suggest that FRET process induced quenching of AO fluorescence emission in mixed ethanol solution. The Froster radius, intermolecular distance and the energy transfer efficiencies at various concentrations of RhB are also summarized in Table 1. It is clearly observed that the FRET efficiency is much higher in aqueous environment than that in ethanol solution. This result basically implies that the excited state dipole interaction essentially depends on the polarity of the solvent i.e., more polar the environment more is the energy migration from donor to the acceptor moieties. Also the FRET here is more pronounced at shorter distances (10–100 Å) between the participating molecular entities.

### 3.3. Effect of clay on the energy transfer between AO and RhB

The effect of clay mineral montmorillonite (MMT) on the fluorescence resonance energy transfer between AO and RhB in the aqueous environment has been studied in the present work for various clay concentrations. The negatively charged clay is used as the host platform on which the cationic dyes are adsorbed via electrostatic interaction. Therefore, to confirm the FRET we first recorded the steady state fluorescence emission spectra of pure AO, pure RhB in the aqueous MMT clay dispersion. It is observed that the shape of their emission spectra are similar except some change of the intensity distribution when compared to that of aqueous solution of dyes in absence of clay. The unaltered emission band at 525 nm and 575 nm for AO and RhB respectively in the mixture may resemble the presence of monomer unit of dye molecules while adsorption onto clay surfaces. The slight decrease in emission intensity is only due to their adsorption onto the clay surface, but not due to any self-quenching of dye molecules as no decrease of emission was observed for dye with higher concentrations in the same clay dispersion. Some researchers [29] reported that the reduction of fluorescence intensity is attributed to the light scattering by the inorganic clay nanosheets in their aqueous dispersion. So in our experiment the scattering of light might have contributed to fluorescence quenching of AO in RhB/clay aqueous dispersion. Then we measured the emission spectra of AO/RhB mixed solution (1:1 vol ratio) with various concentrations of RhB (similar as before) in presence of clay nanoplatelets. The clay concentration was considered as 2 ppm and 4 ppm in each set of experiment and the corresponding emission spectra are shown in Fig. 3A and B.

From Fig. 3A and B it is clearly observed that the fluorescence emission band at 525 nm (AO) for the mixed ensemble in the aqueous clay dispersion decreases gradually with increase in RhB concentrations and correspondingly the emission intensity at 575 nm increases. For both the clay concentrations (2 ppm and 4 ppm) this systematic manifestation of emission intensity corresponds an energy transfer process due to the resonance coupling of the oscillating dipoles of the excited fluorophores. The efficiency of this energy migration from donor to acceptor molecules in presence of clay nanoplatelets is summarised in Table 2. Interestingly the presence of clay in the mixed dye solution enhanced the energy transfer efficiency at lower concentrations of RhB in the solution, but in higher concentrations it is less in absence of clay. Additionally, the Froster radius in presence of clay is somewhat decreased when compared to that of AO-RhB mixed solution without clay.

**Table 1**Average overlap integral ( $J(\lambda)$ ), Förster distance ( $R_0$ ), energy transfer efficiency (E) and center to center distance (r) between AO & RhB of different concentrations of RhB in water & ethanol solvent.

Acceptor solution	In water: $J(\lambda) = 3.89483 \times 10^{15} \text{ nm}^4 \text{ M}^{-1} \text{ cm}^{-1}$ ( $R_0 = 34.705 \text{ \AA}$ )		In ethanol: $J(\lambda) = 5.47293 \times 10^{15} \text{ nm}^4 \text{ M}^{-1} \text{ cm}^{-1}$ ( $R_0 = 54.32 \text{ \AA}$ )	
	Concentration of RhB (M)	E (%)	r (Å)	E (%)
$10^{-7}$	10	49.60	1	116.83
$2 \times 10^{-7}$	11	49.17	2	103.91
$5 \times 10^{-7}$	12	48.37	5	88.73
$7 \times 10^{-7}$	13	47.64	4	92.26
$10^{-6}$	14	46.97	6	85.92
$2 \times 10^{-6}$	21	42.98	9	79.87
$4 \times 10^{-6}$	24	42.06	7	83.60
$6 \times 10^{-6}$	26.5	41.14	12	75.71
$8 \times 10^{-6}$	34	38.76	25	65.23
$10^{-5}$	43	36.37	32	61.59

The distances between FRET pair at every RhB concentration are also gradually decreased compared to that in absence of clay, which facilitate enhanced rate of energy transfer between AO and RhB in aqueous clay dispersion. It is important to emphasize here that smectite type of clay particulates have negative charge on their layered surface and is generally balanced due to the presence of cations namely Na, Ca, Mg and H in the interlayer region. In aqueous dispersion these cations are displaced due to swelling properly and effectively individual clay nanosheets become negatively charged. Here in this work both AO and RhB are cationic dyes and become positively charged in their aqueous solution. As a result, when mixed with clay dispersion they could eventually adsorbed onto the clay surface due to their cation exchange properties. Also due to the adsorption of dye molecules onto the clay surfaces they are more restricted and come closer to each other compared to solution where they are relatively free resulting the increase of FRET efficiency due to strong intermolecular dipolar coupling between donor and acceptor. Therefore, it can be conducted that the MMT plays an important role to assemble the dye molecules at their surfaces resulting a noticeable decrease of intermolecular separation of AO and RhB. This in turn favours the condition of more efficient energy migration in the excited state of the dye molecules. It is also interesting that the energy transfer between AO and RhB in their dilute aqueous solution in presence of clay nanoparticles is appreciable because the donor-acceptor distance lies in the range 10–100 Å for all clay concentrations used in this study and the distance gradually decreases with increase in clay concentrations.

We have already seen that the energy transfer efficiency is largely influenced by the amount of clay in the AO/RhB mixed solution. However, it is also significant that the FRET efficiency depends on the acceptor (RhB) concentration for particular fixed concentration of donor AO and MMT clay. From Table 2 it is further clear that for RhB concentration of  $8 \times 10^{-6}$  the FRET efficiency is maximum when clay concentration was 2 ppm. From Fig. 3C we immediately observe that FRET efficiency is almost linear with different varying concentrations of RhB in absence and presence of clay (2 ppm). But for higher clay concentration (4 ppm) the plot initially shows straight line for few concentrations of RhB and then starts to deviate from the linearity. That is at higher acceptor concentrations the FRET efficiency tends to decrease slightly. This is because of the fact that when the concentration of RhB is high, the dye molecules tend to form aggregates which may affect the excitation energy thereby reducing the number of acceptor molecules participating the resonant interaction with AO molecules after photoexcitation. The energy transfer between AO and RhB in presence of MMT clay is schematically shown in Fig. 4.

In the present work we have also tested the energy transfer process for fixed amount of AO (donor) and RhB (acceptor) for different various concentrations of clay dispersion in the mixed dye solution. Fig. 5A shows the steady state fluorescence emission spectra of AO/RhB mixed solution (1:1 vol ratio) at different clay concentrations namely 2 ppm, 4 ppm, 6 ppm, 8 ppm and 10 ppm. From the figure it is observed that with increase in clay concentrations, the emission band with peak at 525 nm is gradually quenched to significant amount with respect to that of pure AO aqueous solution. Although the emission band intensity at 575 nm is decreased as the clay concentration is increased but the ratio of the intensity of the bands at 575 nm and 525 nm is increased linearly as illustrated in the inset of Fig. 5A. This essentially confirms the gradual increase of energy transfer from excited AO to RhB molecules with increase of clay platelets in the mixture. However, the absolute decrease of steady state fluorescence band intensity at 575 nm might be due to formation of non-fluorescent dye aggregates after addition of clay platelets in the mixture. More precisely the total number of dye monomer units might have increased with increase in clay concentration. But this reduction is relatively less compared to the enhancement of emission intensity at 575 nm due to FRET process when clay concentration is increased. Also the FRET efficiency between AO and RhB increases linearly with increase in clay concentration as shown in Fig. 5B and the FRET efficiency reached to 62.48% at clay concentration of 10 ppm. The corresponding change in FRET efficiency is summarised in Table 3.

To reveal the nature of the quenching mechanism of the fluorescence emission of the donor fluorophores in presence and absence of acceptor, the Stern-Volmer (S-V) relation [30] has been applied and is given by

$$F_0/F = 1 + K_{SV}[Q] \quad (8)$$

where  $F_0$  and  $F$  denote the steady-state fluorescence emission intensities of donor (AO) in the absence and presence of quencher molecules (RhB), respectively.  $K_{SV}$  is the Stern-Volmer quenching constant and  $[Q]$  is the concentration of quencher. The Stern-Volmer plot as obtained from the steady state fluorescence emission results for mixed solution of AO and RhB as well as for pure AO in aqueous media is almost straight line (Fig. 6A). The linearity in S-V plot suggests that the quenching may be of either pure dynamic or pure static nature. Generally, deviations from linearity indicate the mixing of both dynamic and static quenching processes [31] and therefore the quenching of AO fluorescence in presence of RhB in ethanolic medium (as shown in Fig. 6B) might be due to both static and dynamic quenching.

On the other hand, the S-V plot as obtained from the steady state fluorescence spectra of AO/RhB mixed aqueous solution in

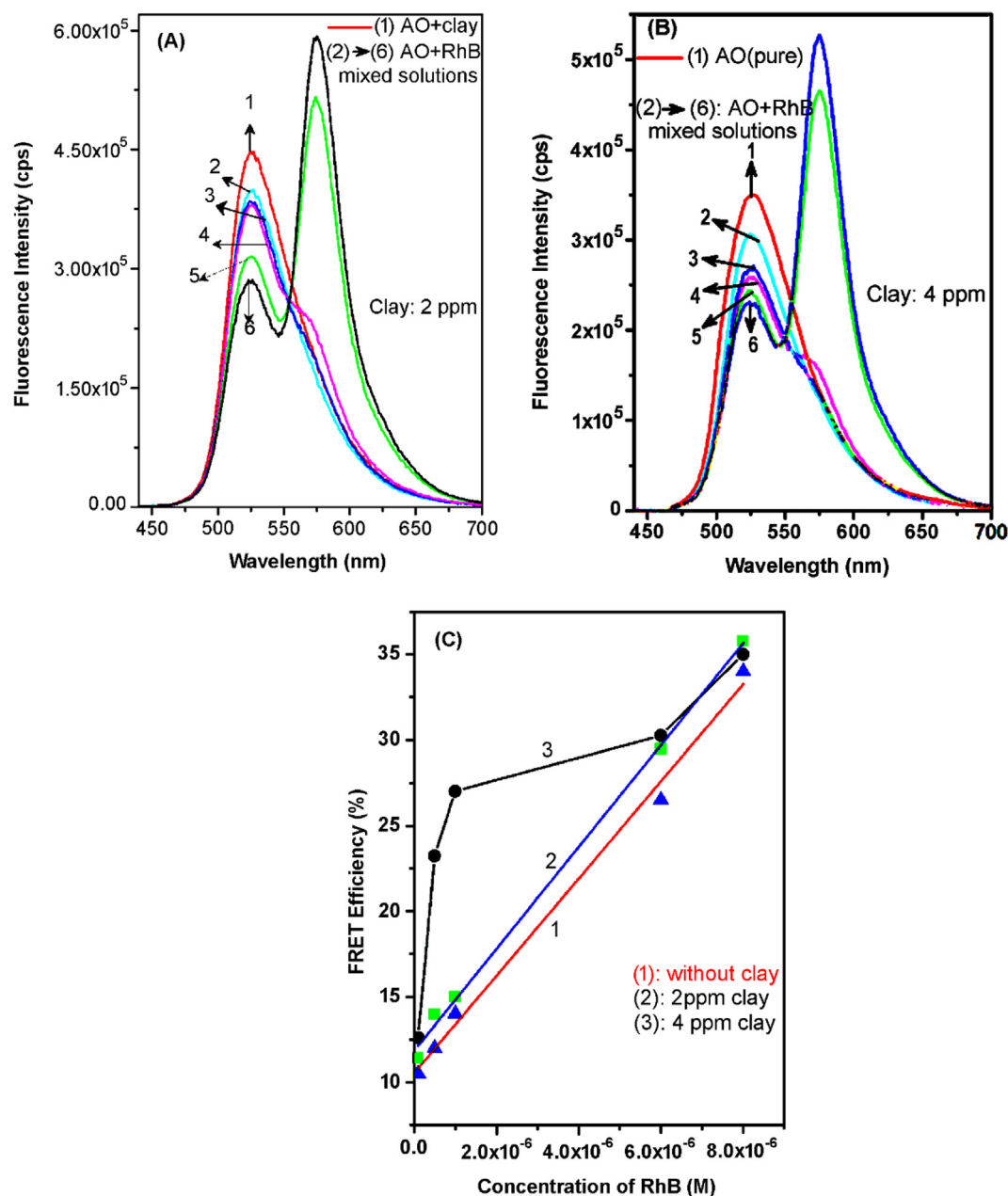


**Fig. 3.** Steady state fluorescence emission spectra of AO/RhB mixed solution (1:1 vol ratio) in presence of MMT clay of concentration of (A) 2 ppm (B) 4 ppm. Concentration of RhB solution was varied with  $10^{-7}$  M,  $5 \times 10^{-7}$  M,  $10^{-6}$  M,  $6 \times 10^{-6}$  M and  $8 \times 10^{-6}$  M for each concentration of MMT clay. Concentration of AO solution was fixed at  $5 \times 10^{-6}$  M in all cases. (C) Variation of FRET efficiency (%) between AO and RhB in absence and presence of MMT clay (2 ppm and 4 ppm) in aqueous medium.

presence of 4 ppm clay dispersion (See Fig. 7) shows almost linearity which also suggests that the fluorescence quenching might be type either static or dynamic quenching. Though static quenching is dominant for the interactions of dyes with clay platelets, some part of fluorescence quenching might be coming from free AO/RhB interaction in solution. Time resolved fluorescence study and temperature dependence fluorescence emission measurements as discussed in the later sections further confirm the quenching behaviour of the donor fluorophores i.e. AO molecules in the mixed dye solution.

#### 3.4. Fluorescence lifetime study by Time-Correlated Single-Photon counting method (TCSPC)

To explore the further knowledge about the nature of fluorescence quenching of donor molecules (AO) in presence of RhB as

well as mixed solution of RhB and MMT clay during the process of excited state energy transfer via FRET among the dye chromophores a time-correlated single-photon counting (TCSPC) study is performed because of the fact that the decay time measurements are more sensitive than steady state fluorescence measurements from the point of view of experimental observations. All the sample solutions were excited at wavelength of 425 nm via laser light while the emission of donor molecules were monitored at wavelength of 525 nm. Fig. 8 shows the fluorescence decay plot of pure aqueous solution of AO (concentration of  $5 \times 10^{-6}$  M), AO/RhB mixed solution in absence and presence of MMT clay. The concentration of RhB and clay were  $4 \times 10^{-6}$  M and 4 ppm respectively for this purpose. The fluorescence decay results as obtained were fitted and analysed with the help of DAS 6 software using two exponentials and the average lifetime of pure AO, AO/RhB mixed solution and AO/RhB/MMT mixed solutions were estimated as

**Table 2**

Average overlap integral ( $J(\lambda)$ ), Fröster distance ( $R_0$ ), energy transfer efficiency ( $E$ ) and centre to centre distance ( $r$ ) between AO and RhB for different concentration of RhB in presence of MMT clay of different concentrations.

Acceptor solution	Clay: 2 ppm, $J(\lambda) = 1.611 \times 10^{15} \text{ nm}^4 \text{ M}^{-1} \text{ cm}^{-1}$ ( $R_0 = 32.08 \text{ \AA}$ )		Clay: 4 ppm, $J(\lambda) = 3.036 \times 10^{15} \text{ nm}^4 \text{ M}^{-1} \text{ cm}^{-1}$ ( $R_0 = 33.30 \text{ \AA}$ )	
	Concentration of RhB (M)	E (%)	$r$ (Å)	E (%)
$10^{-7}$	11.4	45.15	12.6	45.99
$5 \times 10^{-7}$	14.0	43.42	23.24	40.64
$10^{-6}$	15.0	42.84	27.0	39.31
$6 \times 10^{-6}$	29.46	37.11	30.26	38.27
$8 \times 10^{-6}$	35.79	35.37	35.0	36.92

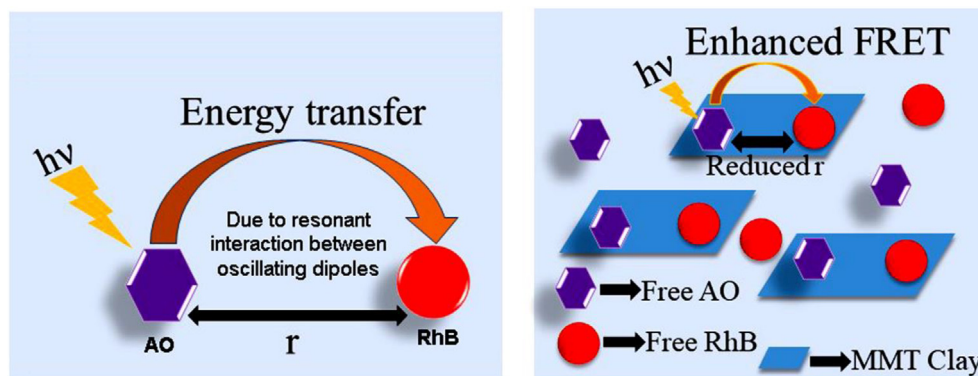


**Fig. 4.** Schematic diagram of the fluorescence resonance energy transfer (FRET) between donor molecules (AO) and acceptor free monomers (RhB) in absence and presence of MMT clay in the aqueous environment. The relative distance between AO and RhB decreases while adsorbed on to clay surface.

1.682 ns, 1.538 ns and 1.70 ns respectively. It is clear from this study that after addition of acceptor molecules i.e. RhB to AO solution the lifetime of AO (donor) is reduced to an appreciable value and therefore the lost excited state energy might have migrated to RhB molecules in a non-radiative mechanism so that there is

an increase of fluorescence intensity of emission peak (at 575 nm) of RhB as is observed from the steady state measurements. So, the fluorescence quenching of AO and the corresponding reduction of their excited state lifetime may be referred to as dynamic or collisional quenching [32]. On the other hand, after

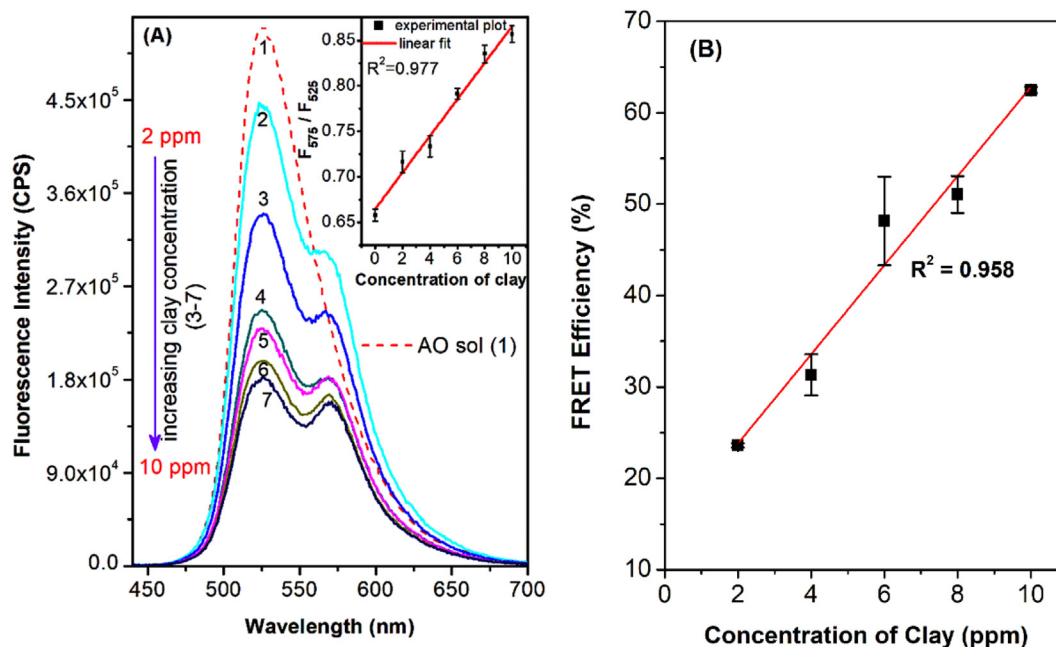


**Fig. 5.** (A) Steady state fluorescence emission spectra of pure AO solution and AO/RhB mixed solution in MMT (1:1:1 vol ratio) clay aqueous dispersion. The concentrations of AO and RhB were  $5 \times 10^{-6} \text{ M}$  and  $4 \times 10^{-6} \text{ M}$  respectively. Concentrations of MMT clay was varied as 0 ppm, 2 ppm, 4 ppm, 6 ppm, 8 ppm and 10 ppm. Inset shows the variation of the ratios of fluorescence intensity of the bands at 575 nm and 525 nm of AO/RhB mixed solution with various concentrations of clay. (B) Variation of FRET efficiency (%) between dye pair as a function of MMT concentrations in the mixed dye solution.

**Table 3**  
Energy transfer efficiencies in presence of MMT clay in aqueous medium.

Clay concentration →	2 ppm	4 ppm	6 ppm	8 ppm	10 ppm
Energy transfer efficiency	23.60%	31.33%	48.16%	51.06%	62.48%

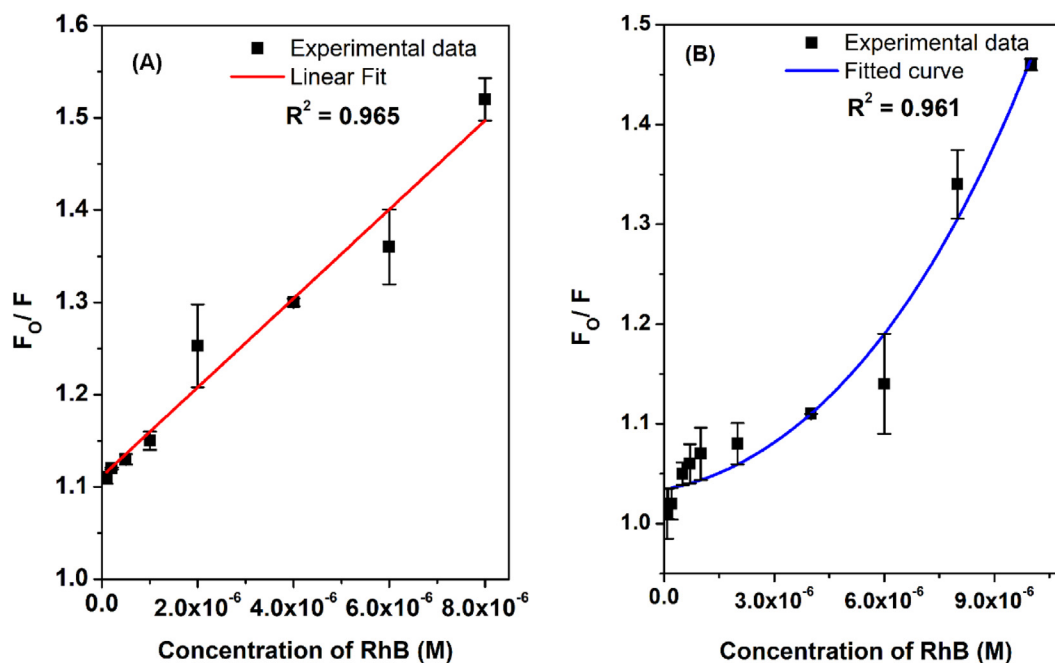


**Fig. 6.** (A) Stern-Volmer Plot as obtained from the fluorescence spectra of AO/RhB mixed solution with various RhB concentration in water and (B) ethanolic solutions at room temperature.

addition of MMT clay dispersion to mixed solution of AO and RhB there is no such appreciable change of fluorescence lifetime and this corresponds to static quenching. Actually in presence of clay the effective distance between AO and RhB molecules decreases which increases the energy transfer efficiency but not all the molecules did not participate in the energy transfer process when compared to that in absence of MMT clay may be because of electrostatic screening between the molecules. In other words, the presence of clay obviously facilitates the energy transfer rate between the excited molecules. However, the almost unaltered fluorescence lifetime may be due to the intrinsic lifetime of AO molecules which were unreacted with RhB molecules because the presence of negatively charged clay platelet restricts the direct random collision between AO and RhB. So static quenching of fluorescence of AO might have occurred in presence of RhB/MMT mixed solution.

### 3.5. Thermodynamic parameters and nature of the binding forces

To explore the nature of interactions of AO and RhB in presence and absence of MMT clay, the value of binding constant and binding sites are calculated from the following equation [3,33,34]:

$$\log\left[\frac{F_0 - F}{F}\right] = \log K_b + n \log[Q] \quad (9)$$

where  $K_b$  is the binding constant which can be estimated from the slope of the  $\log[(F_0 - F)/F]$  versus  $\log[Q]$  curve. The values for binding constant ( $K_b$ ) and binding sites  $n$  can be obtained from the intercept and slope of the linear plot as shown in the Fig. 9. To understand this fact, the temperature-dependent fluorescence studies for FRET between AO and RhB in presence and absence of MMT

have been carried out. Concentration of clay aqueous suspension was 4 ppm in this study. Table 4 and 5 show the parameters as obtained from emission measurements at three different temperatures, 15 °C (288 K), 25 °C (298 K), 35 °C (308 K) for AO/RhB and AO/RhB/Clay mixed solutions in aqueous media. From Table 4 it is evident that  $K_b$  and  $n$  increase with increase in temperature which indicates the collisional or dynamical quenching of AO donor molecule, because in dynamical quenching, collision rate generally increases with increase in temperature. However, for AO/RhB/Clay mixed solution (Table 5),  $K_b$  decreases with increase in temperature. This reveals the formation of an unstable compound which corresponds to the static nature of quenching because binding constant between AO and RhB molecules systematically decreases with increase in temperature.

In general, the different types of interactions between small molecules may be originated from various types of forces: viz. hydrogen bonds, van der Waals force, electrostatic interactions, and hydrophobic interaction. Based on the data of enthalpy and entropy change, the type of interactions involved in a close proximity of the molecular species may be concluded as [33,34]:

- (1)  $\Delta H > 0$  and  $\Delta S > 0$ , hydrophobic forces;
- (2)  $\Delta H < 0$  and  $\Delta S < 0$ , van der Waals interactions and hydrogen bonds;
- (3)  $\Delta H < 0$  and  $\Delta S > 0$ , electrostatic interaction.

where  $\Delta H$  is the change of enthalpy and  $\Delta S$  is the change of entropy of AO/RhB mixed ensemble. If the change in enthalpy does not vary significantly with the change in temperature as studied, then its value as well as the entropy can easily be obtained from the well-known van't Hoff equation:



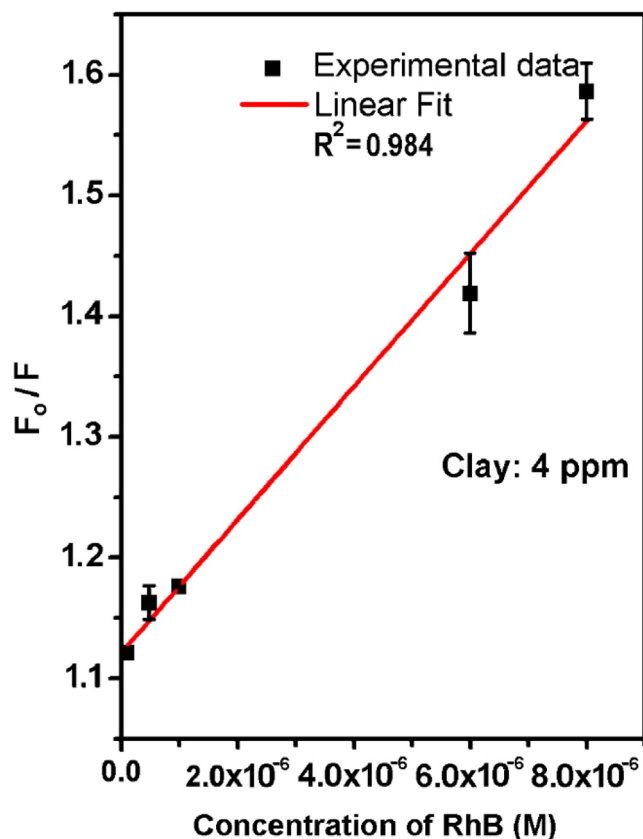


Fig. 7. Stern-Volmer plot as obtained from the fluorescence spectra of AO/RhB mixed solutions in presence of MMT clay of concentration of 4 ppm at room temperature.

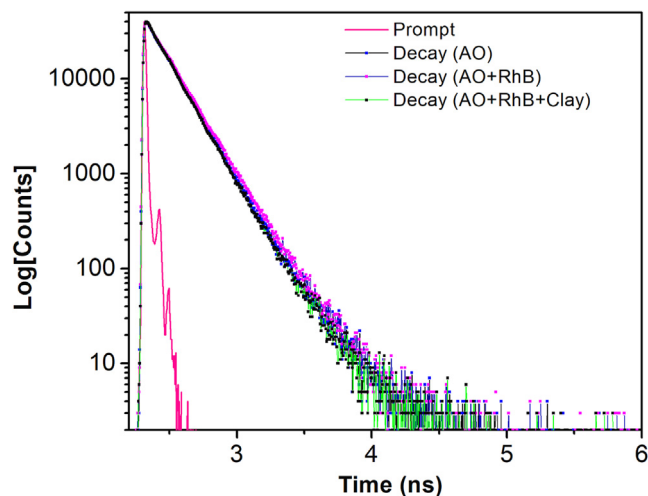


Fig. 8. Fluorescence decay plot of pure aqueous solution of AO, AO/RhB mixed solution in presence and absence of MMT clay aqueous dispersion. All the samples were excited by laser source at wavelength of 425 nm (i.e. near maximum excitation peak of acceptor molecules) and the corresponding fluorescence emission was monitored at 525 nm.

$$\ln K = \frac{\Delta S}{R} - \frac{\Delta H}{RT} \quad (10)$$

Here  $K$  is analogous to the binding constant  $K_b$  at the corresponding temperature and  $R$  is the universal gas constant. The change in Gibbs free energy can be obtained from the following theoretical relation:

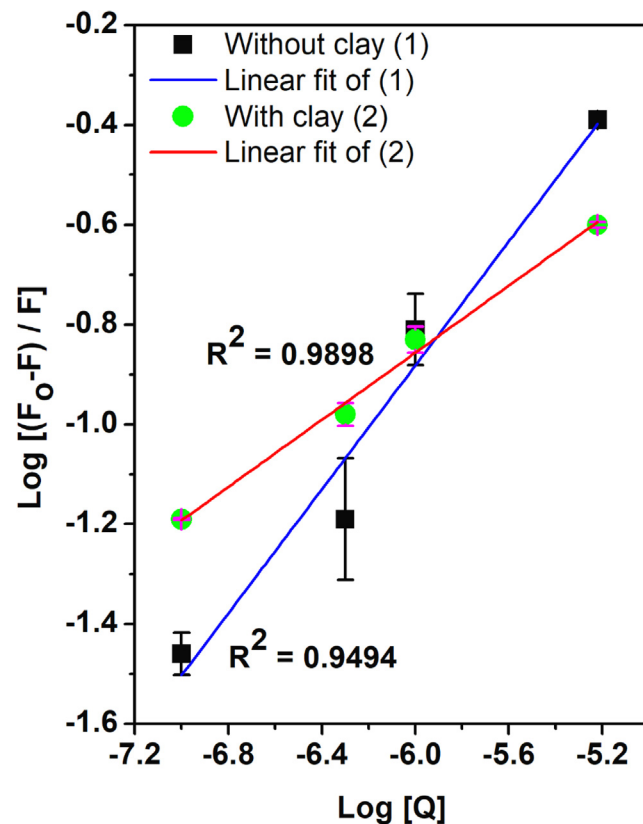


Fig. 9. Plot of  $\log[(F_0-F)/F]$  versus  $\log[Q]$  as obtained from the temperature-dependent steady-state fluorescence measurements where  $F$  is the fluorescence intensity of AO in presence of RhB of various concentrations and  $F_0$  is that of pure AO solution.  $[Q]$  are concentrations of the quencher molecules (RhB).

$$\Delta G = \Delta H - T\Delta S = -RT \ln K \quad (11)$$

From the plot of  $R[\ln K]$  versus  $1/T$  as shown in Fig. 10, the value of  $\Delta H$  &  $\Delta S$  are obtained and hence  $\Delta G$  from the above equation and are summarized in Table 4 and 5. The negative  $\Delta G$  value for both the cases (i.e. AO/RhB and AO/RhB/Clay mixed solution) indicate that the process of interactions is spontaneous.

However, in case of AO/RhB mixed ensemble without clay, both positive values of  $\Delta H$  &  $\Delta S$  reveal that the nature of this interaction is hydrophobic. As both the dyes are cationic in aqueous solution, so electrostatic interaction cannot be responsible for their close proximity for FRET to occur. On the other hand, they are not forming any ground state complex as the mixture is collisional in nature, interaction is mainly due to hydrophobic forces. This is also consistent with the results of the fluorescence lifetime study, where lifetime of AO is decreased after addition of RhB solution.

But in case of AO/RhB/Clay mixed solution, both the negative values of  $\Delta H$  and  $\Delta S$  indicate that the nature of this interaction is due to van der Waals type and hydrogen bonds, that again confirms the formation of ground state complex, where no change of fluorescence lifetime of AO was observed after addition of RhB and clay in the aqueous solution. Therefore, the temperature dependent fluorescence studies of the dye molecules in absence and presence of clay nanoplatelets successfully explain the nature of interaction involved in their close proximity which enables FRET to occur after photoexcitation with light of suitable wavelength.

#### 4. Conclusion

In summary, we have studied the fluorescence emission spectra of cationic dyes AO and RhB both in aqueous solution, ethanol solu-

**Table 4**  
Binding constant ( $K_b$ ), binding sites ( $n$ ), and relative thermodynamic parameters viz. Enthalpy ( $\Delta H$ ), Entropy ( $\Delta S$ ), Gibbs Free Energy ( $\Delta G$ ) at different temperature as obtained from fluorescence spectroscopic data for AO/RhB mixed aqueous solution without MMT clay.

Temperature of AO/RhB mixed solution ( $^{\circ}\text{C}$ )	$K_b$ ( $\text{M}^{-1}$ )	$n$	$R^2$ §	$\Delta H$ ( $\text{kJ M}^{-1}$ )	$\Delta G$ ( $\text{kJ M}^{-1}$ )	$\Delta S$ ( $\text{J K}^{-1}$ )
15	78.86	0.38	0.75	82.072	-10.12	320.109
25	162.92	0.42	0.85		-13.31	
35	691.83	0.62	0.95		-16.52	

§  $R^2$  is the correlation coefficient.

**Table 5**  
Binding constant ( $K_b$ ), binding sites ( $n$ ), and relative thermodynamic parameters viz. Enthalpy ( $\Delta H$ ), Entropy ( $\Delta S$ ), Gibbs Free Energy ( $\Delta G$ ) at different temperature as obtained from fluorescence spectroscopic data of AO/RhB/MMT Clay mixed aqueous solution (4 ppm).

Temperature of AO/RhB (mixed solution ( $^{\circ}\text{C}$ ))	$K_b$ ( $\text{M}^{-1}$ )	$n$	$R^2$ §	$\Delta H$ ( $\text{kJ M}^{-1}$ )	$\Delta G$ ( $\text{kJ M}^{-1}$ )	$\Delta S$ ( $\text{J K}^{-1}$ )
15	38.02	0.41	0.92	-36563.63	-8.63	-96.98
25	20.61	0.56	0.97		-7.66	
35	14.45	0.33	0.99		-6.69	

§  $R^2$  is the correlation coefficient.

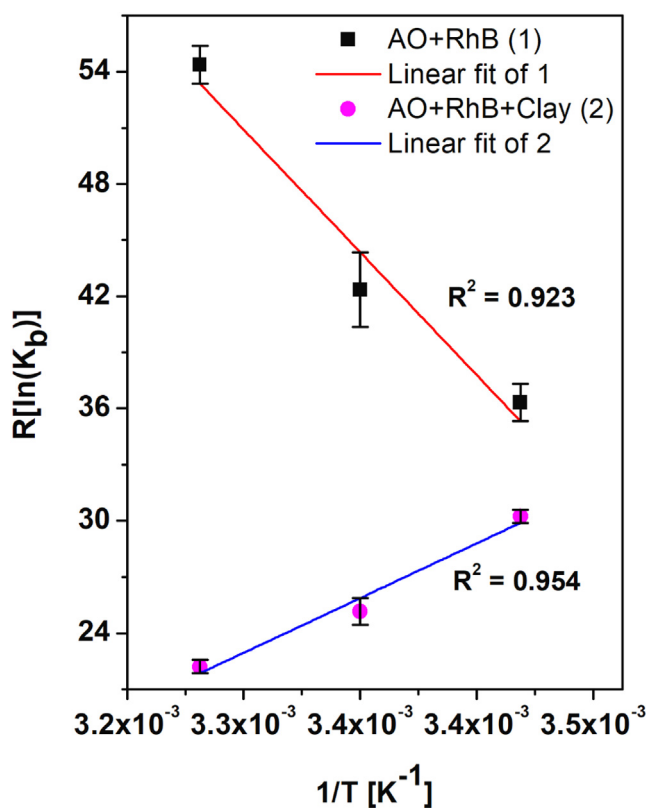


**Fig. 10.** Plot  $R[\ln K_b]$  versus reciprocal ( $1/T$ ) of absolute temperatures at which the corresponding fluorescence emission spectra were measured.  $K_b$  is the value of binding constant of dye molecules at various temperatures as estimated from Fig. 9.

tion and in MMT clay dispersed medium in the aqueous environment and experimentally confirmed the FRET between AO and RhB. The two cationic dyes become excellent pair for FRET to occur because of the sufficient spectral overlap between absorption spectrum of acceptor RhB and fluorescence emission spectrum of energy donor AO. FRET efficiency become relatively much higher in aqueous environment compared to that in ethanol medium for the same set of concentration of AO and RhB in both the media and this implies that the excited state dipole interaction is essentially depends on the polarity of the solvent. That is more polar the environment more is the energy migration from donor to the acceptor moieties. Most interestingly presence of MMT clay in

the mixed dye solution increases the FRET efficiency by reducing the intermolecular distance between AO and RhB in the mixed ensemble. Also energy transfer efficiency increases linearly with increase in clay concentration. The quenching of fluorescence of AO during non-radiative energy transfer from AO to RhB molecules in the excited state in absence of clay is basically due to dynamic or collisional quenching because of reduced fluorescence lifetime of AO. But in presence of clay the dye molecules form ground state complex and the quenching mechanism might be static due to almost similar lifetime of AO as observed by TCSPC fluorescence lifetime measurements. Thermodynamical parameters as estimated by temperature dependent fluorescence study clearly reveal the nature of interactions for the dye molecules in absence and presence of clay platelets. The present study is of significant fundamental importance because of their implication to design FRET-based nano-biosensors to probe various molecular recognition processes.

#### CRediT authorship contribution statement

**Utsav Chakraborty:** Investigation, Methodology, Formal analysis, data curation, Writing - original draft. **Pradip Maiti:** Investigation, Formal analysis. **Tanmoy Singha:** Investigation. **Ujjal Saren:** Investigation. **Alapan Pal:** Formal analysis. **Pabitra Kumar Paul:** Conceptualization, Resources, Supervision, validation, Writing - original draft, writing - review & editing, Funding acquisition, Methodology, Visualization, Project administration.

#### Declaration of Competing Interest

The authors declare that they have no known competing financial interests or personal relationships that could have appeared to influence the work reported in this paper.

#### Acknowledgements

Author P.K. Paul is grateful to DST-SERB of the Government of India for providing major financial assistance through research Project (Grant Ref. No. SB/EMEQ-142/2014) to perform the present work. Authors P.K. Paul and P. Maiti are thankful to West Bengal State Council of Science and Technology for financial assistance via Project (Grant Ref. No. 10 493/WBSCST/F/0545/15(Pt-I)). P.K. Paul is also grateful to Jadavpur University for providing some financial assistance through RUSA 2.0 sponsored Project (Grant Ref. No. R-11/604/19) for the present work.

## References

- [1] J.R. Lakowicz, Principles of Florescence Spectroscopy Chap. 13 (2010) 13.
- [2] D. Dey, D. Bhattacharjee, S. Chakraborty, S.A. Hussain, Sens. Actuat. B Chem. 184 (2013) 268–273.
- [3] G. Mandal, M. Bardhan, T. Ganguly, J. Phys. Chem. C 115 (2011) 20840–20848.
- [4] J. Otten, N. Tenhaef, R.P. Jansen, J. Döbber, L. Jungbluth, S. Noack, M. Oldiges, W. Wiechert, M. Pohl, Microb. Cell. Fact. 18 (2019) 143, <https://doi.org/10.1186/s12934-019-1193-y>.
- [5] K.E. Sapsford, L. Berti, I.L. Medintz, Angew. Chem. Int. Ed. 45 (2006) 4562–4588.
- [6] C.G. dos Remedios, M. Miki, J. Barden, J. Muscle Res. Cell Motility 8 (1987) 97–117.
- [7] D. Dey, D. Bhattacharjee, S. Chakraborty, S.A. Hussain, J. Photoch. Photobio. A 252 (2013) 174–182.
- [8] P.S. Eis, D.P. Millar, Biochemistry 32 (50) (1993) 13852–13860.
- [9] A. Harriman, R. Ziesel, Photochem. Photobiol. Sci. 9 (2010) 960–967.
- [10] J. Saha, A.D. Roy, D. Dey, D. Bhattacharjee, P.K. Paul, R. Das, S.A. Hussain, Spectrochim. Acta A 175 (2017) 110–116.
- [11] W. Chesworth et al., Clay-organic interactions, in: W. Chesworth (Ed.), Encyclopedia of Soil Science. Encyclopedia of Earth Sciences Series, Springer, Dordrecht, 2008. DOI: [https://doi.org/10.1007/978-1-4020-3995-9\\_111](https://doi.org/10.1007/978-1-4020-3995-9_111).
- [12] M. Jaber, J.F. Lambert, S. Balme, Protein adsorption on clay minerals, 2018. DOI: 10.1016/B978-0-08-102432-4.00008-1.
- [13] U. Chakraborty, T. Singha, R.R. Chianelli, C. Hansda, P.K. Paul, J. Lumin. 187 (2017) 322–332.
- [14] J.M. Huggett, Clay Minerals, book chapter in: Reference Module in Earth Systems and Environmental Sciences, 2015. <http://dx.doi.org/10.1016/B978-0-12-409548-9.09519-1>.
- [15] C.R. Reddy, Y.S. Bhata, G. Nagendrappab, B.S. Jai Prakash, Catal. Today 14 (2009) 157–160.
- [16] J.C. Stockert, P.D. Castillo, A. Blázquez-Castro, Acta Histochem. 113 (2011) 668–670.
- [17] B. Zhou, Y.T. Chen, X.L. Zhen, L. Lou, Y.S. Wang, Q.L. Suo, Gold Bull. 51 (2018) 145–151.
- [18] S.A. Hussain, S. Chakraborty, D. Bhattacharjee, R.A. Schoonheydt, Spectrochim. Acta A 75 (2010) 664–670.
- [19] V. Dryza, E.J. Bieske, J. Phys. Chem. C 118 (2014) 19646–19654.
- [20] J. Bhattacharjee, S.A. Hussain, D. Bhattacharjee, Spectrochim. Acta A 116 (2013) 148–153.
- [21] L. Antonov, G. Gergov, V. Petrov, M. Kubista, J. Nygren, Talanta 49 (1999) 99–106.
- [22] S.A. Hussain, S. Banik, S. Chakraborty, D. Bhattacharjee, Spectrochim. Acta A 79 (2011) 1642–1647.
- [23] N.O. Mchedlov-Petrosyan, Y.V. Kholin, Russ. J. Appl. Chem. 77 (2004) 414–422.
- [24] T. Förster, Discuss. Faraday Soc. 27 (1959) 7–17.
- [25] J. Perrin, C.R. Acad. Sci. (Paris) 184 (1927) 1097.
- [26] S. Fery-Forgues, D. Lavabre, J. Chem. Educ. 76 (1999) 1260–1264.
- [27] M.S.C.J.R. Bolton, Photochem. Photobiol. 34 (1981) 537547
- [28] D. Ghosh, D. Bose, D. Sarkar, N. Chattopadhyay, J. Phys. Chem. A 113 (2009) 10460–10465.
- [29] A. Czimerová, J. Bujdak, N. Iyi, J. Photochem. Photobiol. A 187 (2007) 160–166.
- [30] M.E.K. Wahba, N. El-Enany, F. Belal, Anal. Methods 7 (2015) 10445–10451.
- [31] J.S. Kadavevarmath, G.H. Malimath, R.M. Melavanki, N.R. Patil, Spectrochim. Acta A 117 (2014) 630–634.
- [32] K.A. Paterson, J. Arlt, A.C. Jones, Methods Appl. Fluoresc. 8 (2020) 025002, <https://doi.org/10.1088/2050-6120/ab71c3>.
- [33] P.D. Ross, S. Subhramanian, Biochemistry 20 (1981) 3096–3102.
- [34] R. Bhattacharya, C.R. Patra, S. Wang, L. Lu, M.J. Yaszemski, D. Mukhopadhyay, P. Mukherjee, Adv. Funct. Mater. 16 (2006) 395–400.